

OPTICAL PROPERTIES OF COMETARY NUCLEI AND A PRELIMINARY COMPARISON WITH ASTEROIDS

DAVID C. JEWITT¹ AND KAREN J. MEECH¹

Department of Earth, Atmospheric, and Planetary Sciences, Massachusetts Institute of Technology

Received 1987 August 20; accepted 1987 October 30

ABSTRACT

Direct CCD observations of cometary nuclei are used to make a preliminary physical comparison with main-belt asteroids of comparable size. The nuclei have been studied within the past 2 yr using charge-coupled devices; the observations of P/Neujmin 1 and P/Tempel 2 are presented here for the first time. The photometric ranges of the nuclei are found to be larger than the ranges of typical main-belt asteroids of similar size, suggesting a systematic shape difference between the nuclei and the small asteroids. The shape difference may be a result of the different collisional histories of the nuclei and asteroids or of anisotropic sublimation of the nuclei. These and other possibilities are briefly discussed. From the scant available information we suspect that the shapes of the nuclei may be more similar to the shapes of Earth-crossing asteroids than to the shapes of main-belt asteroids, consistent with, but not proving, a common origin for the cometary nuclei and the Earth-crossing asteroids. While even the most elongate nuclei are gravitationally bound, several are found to be rotating near the centripetal limit for bulk densities of order $100\text{--}200\text{ kg m}^{-3}$.

Subject headings: asteroids — comets

I. INTRODUCTION

Measurements of the physical properties of cometary nuclei hold special interest, since they refer to a set of primitive bodies which, unlike the asteroids, may have remained thermally and collisionally unevolved since the time of their formation. The nuclei may be some of the original planetesimals from which the outer planets and satellites were formed. Thus, the comets may yield clues about the physical nature of the planetesimals and provide a reference against which the collisional modification of the asteroids may be judged.

Until recently, direct ground-based observations of the nuclei of comets were held to be impossible, since comets bright enough to be observed with traditional photometers are usually sufficiently close to the Sun to possess extensive comae. The cross section in the typical coma is orders of magnitude larger than the (few km^2) cross section of the typical nucleus, so that the fractional contribution to the scattered light from the nucleus is very small. For this reason, very few observations of cometary nuclei have been attempted; even fewer have been reported. However, we have found that charge-coupled devices (CCDs) can be used to detect and examine the nuclei of certain comets, specifically, comets at very large heliocentric distances and weakly active comets at smaller distances. We employ observational techniques similar to those used by others for the photometric study of asteroids, but the objects of our attention are about 100 times fainter than the commonly studied asteroids.

Observations of the first three nuclei observed by us with CCDs are already published. Comet P/Arend-Rigaux (Jewitt and Meech 1985), a low-activity nucleus, was observed at heliocentric distance $R = 1.54\text{ AU}$. The nucleus was embedded in a faint dust coma; CCD area photometry was used to subtract the coma and to determine several nucleus properties.

P/Halley (Jewitt and Danielson 1984; Meech, Jewitt, and Ricker 1986) was observed at distances ($6 \leq R \leq 11\text{ AU}$) beyond the water sublimation zone. The photometry was consistent with detection of a bare nucleus, and the published properties of the nucleus derived from the CCD data were in good agreement with subsequent *in situ* measurements from spacecraft (Sagdeev *et al.* 1986; Keller *et al.* 1986). Under-sampling prevented the determination of the rotation period, although periods $P < 18\text{ hr}$ were ruled out. P/Encke (Jewitt and Meech 1987) was observed near aphelion ($R = 4\text{ AU}$). The comet appeared stellar, and had a cross section equal to the radar cross section within the uncertainties of measurement. The nucleus was found to be significantly aspherical, and the rotation period was estimated.

Related observations of P/Arend-Rigaux have been reported by Tokunaga and Hanner (1985), Brooke and Knacke (1986), Millis, A'Hearn, and Campins (1987), and Birkett *et al.* (1987) and of P/Neujmin 1 by Birkett *et al.* (1987) and by Campins, A'Hearn, and McFadden (1987), using near simultaneous data at optical and thermal infrared wavelengths. The main advantage of the optical/IR approach is that the nucleus albedo and cross section can be measured separately, whereas CCD photometry alone yields only their product. The main disadvantage is that precise thermal infrared photometry is generally possible only on optically bright objects (say, $V \leq 17\text{--}18$) which are more likely to possess coma. In addition, the infrared detectors so far employed lack spatial resolution, making detection and rejection of residual coma more difficult than with a CCD. Presumably, the most complete understanding of nuclei will come from the CCD and optical/IR methods combined.

In the following sections, we describe our study of the 4th and 5th CCD nuclei, comets P/Neujmin 1 and P/Tempel 2, and we make a preliminary comparison of the properties of the nuclei with the properties of small asteroids, all measured using similar ground-based photometric techniques. Possible physical differences between the nuclei and the asteroids are emphasized. We hope that the present work will stimulate further

¹ Visiting Observer at the Kitt Peak National Observatory, National Optical Astronomy Observatories, operated by the Association of Universities for Research in Astronomy, Inc., under contract with the National Science Foundation.

research into the shapes and rotational properties of comets and small asteroids.

II. OBSERVATIONS

a) Comet P/Neujmin 1

Comet P/Neujmin 1 (orbital period 18.2 yr, eccentricity 0.776, inclination 14°2) is one of the least intrinsically active of the known comets. It exhibits a faint coma near perihelion (heliocentric distance $R = 1.55$ AU), and a tail is occasionally apparent, but in many instances the comet appears "stellar," suggesting that the bare nucleus may sometimes be observed. The geometric albedo of the nucleus is estimated at $p_v = 0.02$ – 0.03 and the radius at $r \approx 10$ km (Campins, A'Hearn, and McFadden 1987). The nongravitational acceleration of this comet is as yet undetected (Marsden 1968), testifying to both the low rate of mass loss and the large size of the nucleus.

Comet P/Neujmin 1 was observed in 1985 September ($R = 3.8$ AU) using the 4 m telescope at Kitt Peak National Observatory (KPNO) and in 1986 March ($R = 5.03$ AU) and 1986 October–November ($R = 6.46$ AU) using the KPNO 2.1 m telescope. A full description of the observing procedures has been given elsewhere (Jewitt and Meech 1987); therefore, we here confine ourselves to a brief account. The observations were taken with a cooled TI 800 \times 800 pixel CCD with an image scale 0".29 per pixel at the 4 m prime focus and 0".38 per pixel at the 2.1 m Cassegrainian focus. Observations were primarily taken through the Mould R filter ($\lambda_c = 6500$ Å, full width at half-maximum [FWHM] = 900 Å), with the telescopes tracking to follow the motion of the comet with respect to the sidereal rate. Typical integrations of 600 s were used on the 2.1 m telescope. Relative photometric calibration of the independent pixels on the CCD was achieved using bias frames and nightly dome flats, while absolute photometric calibration was obtained from observations of selected standard star fields (Christian *et al.* 1985). The geometrical properties of the comet on each date of observation are listed in Table 1.

During all three observing runs comet P/Neujmin 1 appeared as a stellar object of magnitude $m_R \approx 18$ – 21 . A representative CCD image is presented in Figure 1a (Plate 15). Photometry was extracted from the CCD images using circular diaphragms with a range of sizes. The data presented in this paper were obtained using a circular photometry diaphragm of 6".1 diameter and a concentric sky annulus with inner and outer diameters 6".1 and 9".1, respectively. Great care was taken to ensure that the comet was free from interference by underlying field objects down to about magnitude $m_R \approx 24$. Specifically, the comet was avoided during those times when any interference was suspected. The results of the photometry are summarized in Table 2. The magnitude errors in Table 2 are

estimates of the uncertainty resulting from noise in the sky near the comet.

Three pieces of observational evidence are consistent with the detection of the bare nucleus of P/Neujmin 1:

1. The surface-brightness profile of the comet is stellar.
2. The apparent magnitudes of P/Neujmin 1 (Table 2) are consistent with an inverse-square dependence on the heliocentric, R , and geocentric, Δ , distances, expressed in magnitudes as

$$m_R = m_R(1, 1, 0) + 5 \log (R \Delta) + \beta \alpha, \quad (1)$$

where α (degrees) is the phase angle and β (magnitudes per degree) is the phase coefficient. The absolute magnitude $m_R(1, 1, 0)$, is listed in the last column of Table 2. The phase coefficient derived from a least-squares fit to the present observations is

$$\beta = 0.034 \pm 0.012 \text{ mag deg}^{-1}, \quad (2)$$

consistent with earlier determinations ($\beta \approx 0.03$ – 0.05 mag deg $^{-1}$) based on photographic magnitudes (Sekanina 1976). Comparably large phase coefficients are observed in dark "C-type" asteroids (Bowell and Lumme 1979), in which the low albedo suppresses multiple scattering among the grains in the regolith. The inverse-square dependence and the large phase coefficient are both consistent with the optical behavior expected of an inert nucleus of low albedo and are quite different from the irregular behavior expected of an active comet.

3. Additional evidence that our photometry refers to the bare nucleus comes from the presence of large cyclic variations in the cometary magnitude, as shown in Figure 2. Analogous rotational variations are known in comets P/Arend-Rigaux, P/Halley, and P/Encke (see § I). The least contrived explanation of these variations is that they are caused by rotation of the nucleus. "String length" (Dworetzky 1983) and χ^2 period searches were applied to the photometry from Table 2. The resulting plot of χ^2 versus ω , the angular frequency of a best-fit sinusoid, is shown in Figure 3. The most significant minimum in χ^2 occurs at $\omega = 0.99$ rad hr $^{-1}$ (light curve period $T = 6.34 \pm 0.05$ hr). By rotational symmetry, we expect the measured light curve period to equal half the nucleus rotation period; therefore, we adopt

$$T = 12.67 \pm 0.05 \text{ hr} \quad (3)$$

as the best estimate of the rotation period of the irregular nucleus. The existence of several adjacent minima in Figure 3 is a result of the undersampling of the light curve in our data. Consequently, it is impossible for us to *prove* which of the minima corresponds to the true rotation period using the existing data. A sinusoid of period $T/2$ has been added to

TABLE 1
GEOMETRY OF COMET P/NEUJMIN 1

Date	Telescope Diameter (m)	Seeing	Number of Observations	R (AU)	Δ (AU)	α
1985 Sep 21	3.8	1".0–2".0	7	3.87	3.97	14°.7
1985 Sep 22	3.8	~1.2	4	3.88	3.96	14.7
1985 Sep 23	3.8	~1.0	4	3.89	3.95	14.7
1986 Mar 06	2.1	~1.3	1	5.04	4.72	11.1
1986 Oct 30	2.1	0.8–1.2	6	6.45	6.29	8.8
1986 Oct 31	2.1	1.6–2.0	5	6.46	6.28	8.8
1986 Nov 01	2.1	1.5	4	6.46	6.26	8.8

TABLE 2
 PHOTOMETRY OF P/NEUJMIN 1

N	Date	UT ^a	Telescope Diameter (m)	Exposure (s)	Time ^b	Air Mass	$m_R \pm \sigma(m_R)$	$m_R(1, 1, 0)^c$
1.....	1985 Sep 21	08:40	3.8	600	08.6655	2.64	18.43 ± 0.05	12.00
2.....	1985 Sep 21	09:10	3.8	300	09.1667	2.14	18.51 ± 0.05	12.08
3.....	1985 Sep 21	09:25	3.8	100	09.4167	1.96	18.56 ± 0.05	12.13
4.....	1985 Sep 21	10:26	3.8	100	10.4333	1.48	18.71 ± 0.05	12.28
5.....	1985 Sep 21	11:34	3.8	50	11.5742	1.20	19.03 ± 0.05	12.60
6.....	1985 Sep 21	11:38	3.8	50	11.6308	1.19	19.06 ± 0.05	12.63
7.....	1985 Sep 21	12:26	3.8	75	12.4258	1.09	19.00 ± 0.05	12.57
8.....	1985 Sep 22	09:44	3.8	100	33.7352	1.74	18.52 ± 0.05	12.09
9.....	1985 Sep 22	10:42	3.8	100	34.7019	1.38	18.52 ± 0.05	12.09
10.....	1985 Sep 22	10:48	3.8	100	34.7947	1.32	18.49 ± 0.05	12.06
11.....	1985 Sep 22	11:28	3.8	100	35.4588	1.20	18.68 ± 0.05	12.25
12.....	1985 Sep 23	09:38	3.8	100	57.6394	1.76	18.81 ± 0.05	12.38
13.....	1985 Sep 23	09:51	3.8	100	57.8508	1.65	18.74 ± 0.05	12.31
14.....	1985 Sep 23	11:01	3.8	150	59.0161	1.29	18.44 ± 0.05	12.01
15.....	1985 Sep 23	11:36	3.8	100	59.6033	1.18	18.42 ± 0.05	11.99
16.....	1986 Mar 06	07:11	2.1	300	07.1836	1.87	19.82 ± 0.07	12.58
17.....	1986 Oct 30	08:18	2.1	600	08.3008	2.16	20.49 ± 0.07	12.15
18.....	1986 Oct 30	09:48	2.1	600	09.7969	1.40	20.69 ± 0.07	12.35
19.....	1986 Oct 30	10:13	2.1	600	10.2086	1.29	20.66 ± 0.07	12.32
20.....	1986 Oct 30	10:43	2.1	600	10.7247	1.19	20.58 ± 0.07	12.24
21.....	1986 Oct 30	11:41	2.1	600	11.6786	1.07	20.41 ± 0.07	12.07
22.....	1986 Oct 30	12:29	2.1	600	12.4864	1.01	20.30 ± 0.07	11.96
23.....	1986 Oct 31	08:42	2.1	600	32.6964	1.83	20.53 ± 0.07	12.19
24.....	1986 Oct 31	09:19	2.1	600	33.3194	1.54	20.39 ± 0.07	12.05
25.....	1986 Oct 31	10:17	2.1	600	34.2786	1.27	20.39 ± 0.07	12.05
26.....	1986 Oct 31	11:31	2.1	600	35.5186	1.08	20.68 ± 0.07	12.34
27.....	1986 Oct 31	11:57	2.1	600	35.9442	1.04	20.74 ± 0.07	12.40
28.....	1986 Nov 01	12:00	2.1	600	60.0011	1.03	20.65 ± 0.07	12.31
29.....	1986 Nov 01	12:11	2.1	600	60.1772	1.02	20.69 ± 0.07	12.35
30.....	1986 Nov 01	12:21	2.1	600	60.3558	1.02	20.61 ± 0.07	12.27
31.....	1986 Nov 01	12:32	2.1	600	60.5356	1.01	20.73 ± 0.07	12.39

^a UT start of integration.

^b Observations (1)–(5)—time in hours since UT 1985 September 21 at 00:00 UT (JD = 2446,329.5).
 Observation (16)—time in hours since UT 1986 March 06 at 00:00 UT (JD = 2,446,495.5).

Observations (17)–(31)—time in hours since UT 1986 October 30 at 00:00 UT (JD = 2,446,733.5).

^c Here $m_R(1, 1, 0) = m_R - 5 \log(R\Delta) - \beta\alpha$; where $\beta = 0.034 \text{ mag deg}^{-1}$.

Figure 2 to visually emphasize the photometric variations in P/Neujmin 1.

The range of the photometric variations seen in Figure 2 is

$$\Delta m = 0.5 \pm 0.1 \text{ mag} . \quad (4)$$

This translates to a rotational variation of the product of the geometric albedo with the cross section of the nucleus of a factor $10^{0.4\Delta m} = 1.6 \pm 0.1$. The albedo of the nucleus has been shown to be independent of rotational phase (Campins, A'Hearn, and McFadden 1987), showing that the light curve is due to irregular shape and not to azimuthal albedo variations. This conclusion is supported by the absence of a rotational variation of the $m_V - m_R$ color of P/Neujmin 1 (see Table 3). We infer that the ratio of the equatorial axes of the nucleus of

P/Neujmin 1 is $a/b \geq 1.6$ (this is a *limit* to a/b because we observe only the projection of the nucleus in the plane of the sky).

The absolute red magnitude of the nucleus at maximum light is $m_R(1, 1, 0) = 12.00 \pm 0.2 \text{ mag}$, where the uncertainty is propagated from equations (1) and (2). The absolute red magnitude of the nucleus averaged over rotational phase is estimated at

$$m_R(1, 1, 0) = 12.25 \pm 0.25 \text{ mag} . \quad (5)$$

The effective radius of the nucleus found from thermal infrared observations varies with time in the range $r = 8.8\text{--}10.6 \text{ km}$ (Campins, A'Hearn, and McFadden 1987). The absolute red magnitude can be combined with the infrared radius to esti-

 TABLE 3
 COLOR OF P/NEUJMIN 1

N	Date	UT	Time ^a	$m_V \pm \sigma_V$	$m_V - m_R \pm \sigma_{V-R}$
1.....	1986 Oct 30	10:01	10.0167	21.15 ± 0.05	0.49 ± 0.07
2.....	1986 Oct 31	08:54	32.9000	20.99 ± 0.05	0.46 ± 0.07
3.....	1986 Oct 31	10:28	34.4667	21.23 ± 0.05	0.55 ± 0.07
4.....	1986 Oct 31	11:45	35.7500	21.24 ± 0.05	0.50 ± 0.07
Mean $m_V - m_R$					0.50 ± 0.04

^a Time in hours since UT 1986 October at 00:00 UT

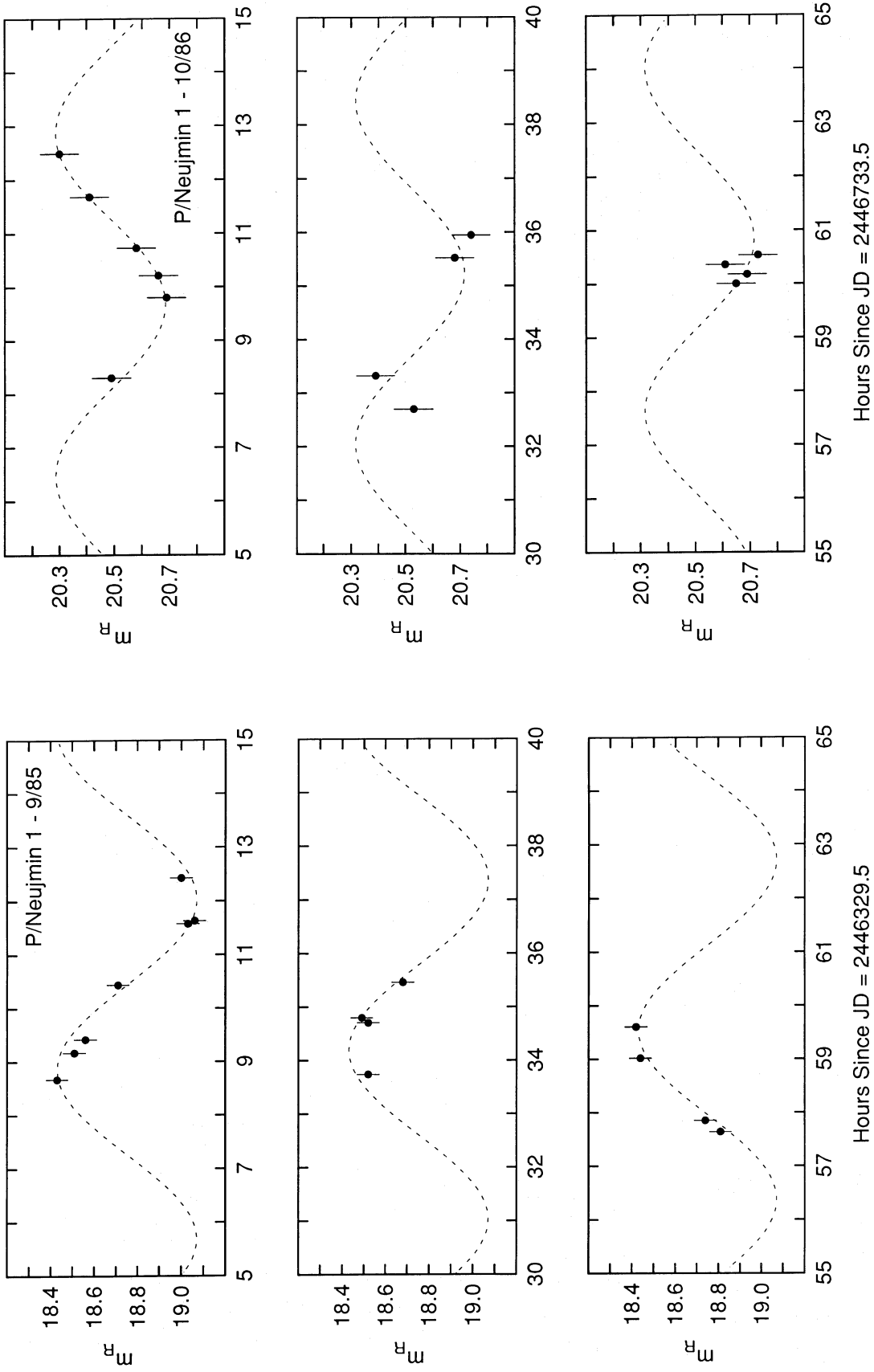


FIG. 2.—(a) and (b) CCD photometry of comet P/Neujmin 1. The plotted data are taken from Table 2. A sinusoid of period $T/2$ has been added to emphasize the periodicity in the photometry. The sinusoid is not a fit to the photometry.

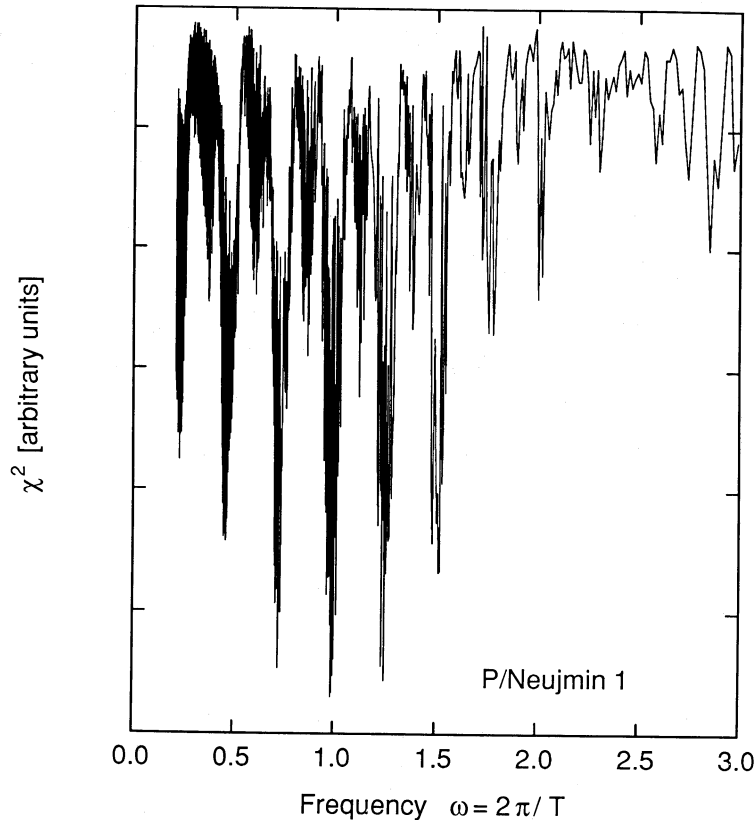


FIG. 3.—Plot of χ^2 versus the angular frequency of the best-fitting sinusoid, for comet P/Neujmin 1 photometry. The best fit corresponds to a two-peaked sinusoid of period $T = 12.67 \pm 0.05$ hr (see text).

mate the red geometric albedo of the nucleus. We obtain

$$P_R = 0.03 \pm 0.01 \quad (6)$$

as the best estimate of the red ($\lambda = 0.65 \mu\text{m}$) geometric albedo of P/Neujmin 1. This is in good agreement with the albedo reported by Campins, A'Hearn, and McFadden. The albedo is equal to the albedo of the nucleus of P/Halley within the uncertainties of measurement. In both cases, the albedo probably refers to a nonvolatile crust on the nucleus, rather than to dirty surface ice.

We note that Wisniewski, Fay, and Gehrels (1986) reported photometric variations with range $\Delta m \approx 0.4$ mag and period 25.44 ± 0.02 hr (equal to $2T$, within the uncertainties of measurement). Their period corresponds to (in our view) an unreasonably complicated light curve with 4 maxima per period. Photometric variations $\Delta m \approx 0.4$ – 0.5 mag were found independently by Campins, A'Hearn, and McFadden (1987) and, although their observations were too sparse to define the period, the variations were apparently consistent with equation (3).

b) Observations of P/Tempel 2

Comet P/Tempel 2 (orbital period 5.29 yr, eccentricity 0.544, inclination $12^\circ.4$, perihelion distance $q = 1.38$ AU) is characterized by its predictable morphological appearance and orbital properties. It has the smallest nonzero nongravitational acceleration of any comet (Yeomans 1978). The transverse component of the acceleration, $A_2 > 0$, indicates prograde rotation of the nucleus, and the stability of A_2 suggests that the rate and angular pattern of the mass loss have been essentially fixed for

at least a century (i.e., precession is small). Several optical outbursts were reported near $R = 3$ AU in the 1979 apparition (Johnson, Smith, and Shorthill, 1981; Barker, Cochran, and Rybski, 1981).

Comet P/Tempel 2 was observed with the Kitt Peak 2.1 m telescope and TI 2 CCD detector on four nights in 1987 March and April, using observational methods the same as those described in § IIa. The comet appeared as a stellar object near $m_R \approx 19.5$ – 19.8 . A representative CCD image is presented in Figure 1b, while the geometrical parameters of the comet are listed in Table 4. Photometry from the CCD images is listed in Table 5 and plotted versus the time of observation in Figure 4. The absolute magnitude listed in Table 5 was computed from equation (1) using $\beta = 0.04 \text{ mag deg}^{-1}$ (Tedesco and Barker 1981).

The comet showed nonrandom photometric variations with a range $\Delta m \approx 0.3$ mag, considerably larger than the estimated ± 0.05 mag photometric uncertainties (Fig. 4). Similar variations were not present in field stars of comparable magnitude, showing that the variations are intrinsic to the comet. The $m_V - m_R$ color of the comet was constant to within the uncertainties of measurement (Table 6).

The χ^2 and string-length period search algorithms were applied to the Tempel 2 photometry. The χ^2 plot is shown in Figure 5. The deepest χ^2 minima occur at angular frequencies $\omega_1 = 1.41 \text{ rad hr}^{-1}$ and $\omega_2 = 1.68 \text{ rad hr}^{-1}$, corresponding to nucleus rotation periods $T_1 = 8.9 \pm 0.1$ hr and $T_2 = 7.5 \pm 0.1$ hr. These minima are separated in frequency by $2\pi/24 \text{ rad hr}^{-1}$ as a result of the periodic sampling forced on the photometry by the day/night cycle. It is tempting to identify the cyclic

TABLE 4
GEOMETRY OF COMET P/TEMPEL 2

Date	Telescope Diameter (m)	Seeing	Number of Observations	R (AU)	Δ (AU)	α
1987 Mar 31	2.1	1"-1.5	10	3.99	3.16	8.9
1987 Apr 01	2.1	~1.1	15	3.99	3.17	9.2
1987 Apr 02	2.1	<1-1.5	11	3.99	3.17	9.4
1987 Apr 03	2.1	~1.1	20	3.98	3.18	9.6

TABLE 5
PHOTOMETRY OF P/TEMPEL 2

N	Date	UT ^a	Telescope Diameter (m)	Exposure (s)	Time ^b	Air Mass	$m_R \pm \sigma(m_R)$	$m_R(1, 1, 0)^c$
1.....	1987 Mar 31	05:49	2.1	300	5.8138	1.02	19.69 ± 0.07	13.83
2.....	1987 Mar 31	05:55	2.1	600	5.9088	1.03	19.70 ± 0.05	13.84
3.....	1987 Mar 31	06:10	2.1	600	6.1669	1.03	19.81 ± 0.05	13.95
4.....	1987 Mar 31	06:32	2.1	600	6.5319	1.05	19.69 ± 0.05	13.83
5.....	1987 Mar 31	07:40	2.1	600	7.6700	1.17	19.48 ± 0.05	13.62
6.....	1987 Mar 31	07:51	2.1	600	7.8467	1.21	19.50 ± 0.05	13.64
7.....	1987 Mar 31	08:12	2.1	600	8.2078	1.28	19.53 ± 0.05	13.67
8.....	1987 Mar 31	08:35	2.1	600	8.5767	1.37	19.59 ± 0.05	13.73
9.....	1987 Mar 31	08:45	2.1	600	8.7517	1.42	19.54 ± 0.05	13.68
10.....	1987 Mar 31	09:46	2.1	600	9.7677	1.90	19.69 ± 0.05	13.83
11.....	1987 Apr 01	03:37	2.1	600	27.6144	1.11	19.62 ± 0.05	13.75
12.....	1987 Apr 01	03:48	2.1	600	27.8000	1.10	19.65 ± 0.05	13.78
13.....	1987 Apr 01	04:11	2.1	600	28.1850	1.06	19.62 ± 0.05	13.75
14.....	1987 Apr 01	06:59	2.1	600	30.9783	1.10	19.53 ± 0.05	13.66
15.....	1987 Apr 01	07:24	2.1	600	31.4139	1.14	19.58 ± 0.05	13.71
16.....	1987 Apr 01	07:36	2.1	600	31.5963	1.18	19.59 ± 0.05	13.72
17.....	1987 Apr 01	07:47	2.1	600	31.7758	1.21	19.62 ± 0.05	13.75
18.....	1987 Apr 01	08:00	2.1	600	32.0025	1.25	19.65 ± 0.05	13.78
19.....	1987 Apr 01	08:11	2.1	600	32.1814	1.29	19.59 ± 0.05	13.72
20.....	1987 Apr 01	08:50	2.1	600	32.8336	1.47	19.67 ± 0.05	13.80
21.....	1987 Apr 01	09:01	2.1	600	33.0183	1.55	19.78 ± 0.05	13.91
22.....	1987 Apr 01	09:12	2.1	600	33.2033	1.63	19.73 ± 0.05	13.86
23.....	1987 Apr 01	09:23	2.1	600	33.3883	1.72	19.68 ± 0.05	13.81
24.....	1987 Apr 01	09:35	2.1	600	33.5763	1.83	19.74 ± 0.05	13.87
25.....	1987 Apr 01	09:46	2.1	600	33.7658	1.97	19.73 ± 0.05	13.86
26.....	1987 Apr 02	03:37	2.1	600	51.6217	1.11	19.73 ± 0.05	13.85
27.....	1987 Apr 02	03:48	2.1	600	51.8014	1.09	19.67 ± 0.05	13.79
28.....	1987 Apr 02	04:37	2.1	600	52.6292	1.03	19.70 ± 0.05	13.82
29.....	1987 Apr 02	05:06	2.1	600	53.0922	1.02	19.64 ± 0.05	13.76
30.....	1987 Apr 02	06:42	2.1	600	54.7025	1.08	19.73 ± 0.05	13.85
31.....	1987 Apr 02	06:53	2.1	600	54.8828	1.09	19.73 ± 0.05	13.85
32.....	1987 Apr 02	07:04	2.1	600	55.0653	1.11	19.75 ± 0.05	13.87
33.....	1987 Apr 02	07:55	2.1	600	55.9206	1.25	19.64 ± 0.05	13.76
34.....	1987 Apr 02	08:06	2.1	600	56.1000	1.29	19.64 ± 0.05	13.76
35.....	1987 Apr 02	08:16	2.1	600	56.2792	1.33	19.63 ± 0.05	13.75
36.....	1987 Apr 02	09:03	2.1	600	57.0533	1.59	19.62 ± 0.05	13.75
37.....	1987 Apr 03	02:46	2.1	600	74.7744	1.22	19.54 ± 0.07	13.64
38.....	1987 Apr 03	02:57	2.1	600	74.9558	1.19	19.64 ± 0.07	13.74
39.....	1987 Apr 03	03:08	2.1	600	75.1331	1.16	19.62 ± 0.07	13.72
40.....	1987 Apr 03	03:21	2.1	600	75.3536	1.14	19.45 ± 0.07	13.55
41.....	1987 Apr 03	03:32	2.1	600	75.5269	1.11	19.54 ± 0.07	13.64
42.....	1987 Apr 03	03:48	2.1	600	75.7919	1.09	19.55 ± 0.07	13.65
43.....	1987 Apr 03	03:58	2.1	600	75.9658	1.07	19.52 ± 0.07	13.62
44.....	1987 Apr 03	04:20	2.1	600	76.3250	1.04	19.62 ± 0.07	13.72
45.....	1987 Apr 03	05:14	2.1	600	77.2292	1.02	19.55 ± 0.07	13.65
46.....	1987 Apr 03	07:26	2.1	600	79.4381	1.17	19.59 ± 0.05	13.69
47.....	1987 Apr 03	07:37	2.1	600	79.6169	1.20	19.56 ± 0.05	13.66
48.....	1987 Apr 03	07:48	2.1	600	79.7953	1.24	19.54 ± 0.05	13.64
49.....	1987 Apr 03	07:59	2.1	600	79.9822	1.28	19.64 ± 0.05	13.74
50.....	1987 Apr 03	08:10	2.1	600	80.1669	1.32	19.60 ± 0.05	13.70
51.....	1987 Apr 03	08:21	2.1	600	80.3475	1.37	19.65 ± 0.05	13.75
52.....	1987 Apr 03	08:32	2.1	600	80.5275	1.42	19.62 ± 0.05	13.72
53.....	1987 Apr 03	08:42	2.1	600	80.7067	1.48	19.69 ± 0.05	13.79
54.....	1987 Apr 03	08:53	2.1	600	80.8859	1.55	19.71 ± 0.05	13.81
55.....	1987 Apr 03	09:04	2.1	600	81.0628	1.63	19.70 ± 0.05	13.80
56.....	1987 Apr 03	09:14	2.1	600	81.2411	1.72	19.69 ± 0.05	13.79

^a UT of the start of the integration.

^b Time in hours since UT 1987 March 31 at 00:00 UT (JD = 2,446,885.5).

^c Here $m_R(1, 1, 0) = m_R - 5 \log(R\Delta) - \beta\alpha$; where $\beta = 0.04 \text{ mag deg}^{-1}$.

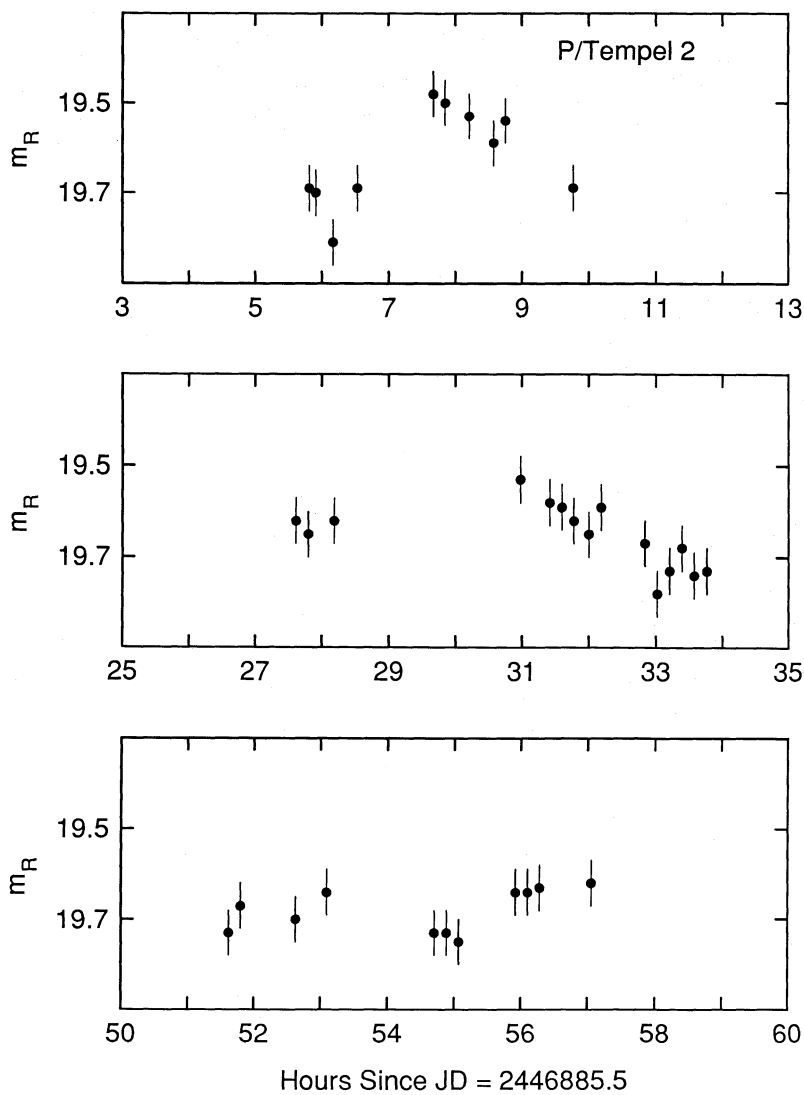


FIG. 4a

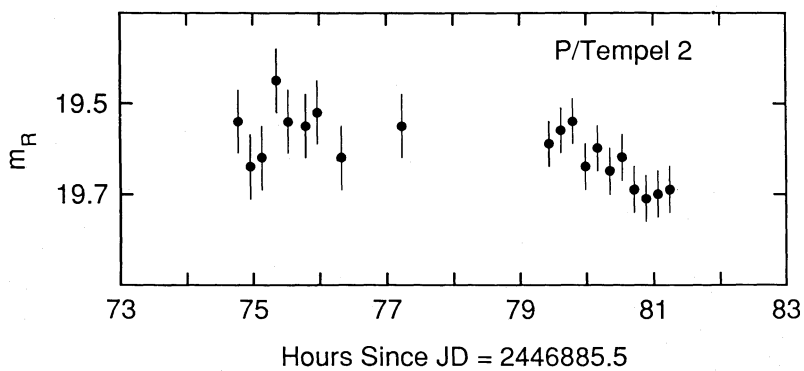


FIG. 4b

FIG. 4.—(a) and (b) CCD photometry of comet P/Tempel 2. The plotted data are taken from Table 5.

TABLE 6
COLOR OF P/TEMPEL 2

N	Date	UT	Time ^a	$m_V \pm \sigma_V$	$m_V - m_R \pm \sigma_{V-R}$
1.....	1987 Mar 31	06:21	6.3528	20.30 ± 0.05	0.55 ± 0.07
2.....	1987 Mar 31	08:02	8.0272	20.05 ± 0.05	0.54 ± 0.07
3.....	1987 Mar 31	08:23	8.3900	20.04 ± 0.05	0.48 ± 0.07
4.....	1987 Apr 01	03:59	27.9911	20.38 ± 0.05	0.59 ± 0.07
5.....	1987 Apr 02	04:49	52.8103	20.16 ± 0.05	0.49 ± 0.07
Mean $m_V - m_R$				0.53 ± 0.03	

^a Time in hours since UT 1987 March 31 at 00:00 UT.

variations in the photometry with the rotation of an aspherical nucleus at one of the state periods. However, neither T_1 , T_2 , nor the several related minima in Figure 5 lead to a convincing light curve, and we do not claim to have detected the rotation period. It is possible that P/Tempel 2 was weakly active at the time of our observations. More photometry is needed to determine whether the suspected periodicities are physically associated with nucleus rotation.

In Table 7, we summarize published photometry of P/Tempel 2, together with absolute magnitudes computed from equation 1, again using $\beta = 0.04 \text{ mag deg}^{-1}$ (Tedesco and Barker 1981). The absolute R filter magnitudes were computed from the published V filter magnitudes assuming $m_V - m_R = 0.5$ (see Table 6). Within the (sometimes considerable) uncertainties of measurement, none of the absolute P/Tempel 2 magnitudes are fainter than the ones we have measured. In this sense, our photometry of Tempel 2 is consistent with a bare nucleus detection. From our photometry alone, we conclude

that the nucleus of P/Tempel 2 has an absolute magnitude not brighter than $m_R(1, 1, 0) = 13.6 \pm 0.1$.

In summary, three pieces of evidence are compatible with, but do not prove, a bare nucleus detection:

1. The surface brightness profile was stellar.
2. The faintest absolute magnitudes of P/Tempel 2 cluster near $m_R(1, 1, 0) \approx 13.6$ –14.0, in observations taken at a range of heliocentric distances in different apparitions (e.g., Johnson, Smith and Shorthill 1981 [$R = 2.97 \text{ AU}$]; Barker, Cochran and Rybski 1981 [$R = 3.32 \text{ AU}$]; Gehrels and Scotti 1987*a, b* [$R = 4.26, 4.19, 4.01 \text{ AU}$]; this work [$R = 3.99 \text{ AU}$]).
3. The peak brightness of the comet in our data is constant from night to night (to $\leq 0.1 \text{ mag}$), even though larger variations ($\Delta m \geq 0.3 \text{ mag}$) are apparent within individual nights. This is precisely the behavior to be expected of a rotating nucleus, but which is not obviously likely to be produced by cometary activity.

Despite these arguments, we remain unconvinced that the bare nucleus of P/Tempel 2 has been observed. Since we are unable to demonstrate the absence of a coma from our photometry, and since we cannot find a convincing rotational light curve, we choose to omit P/Tempel 2 from the following discussion of nucleus properties.

III. DISCUSSION

The photometric parameters of the comet nuclei which we have studied using CCD photometry are summarized in Table 8. The Table lists the absolute red magnitude of each nucleus, $m_R(1, 1, 0)$, the photometric range, Δm , and the probable rotation period, T , where known. In addition, we list the optical

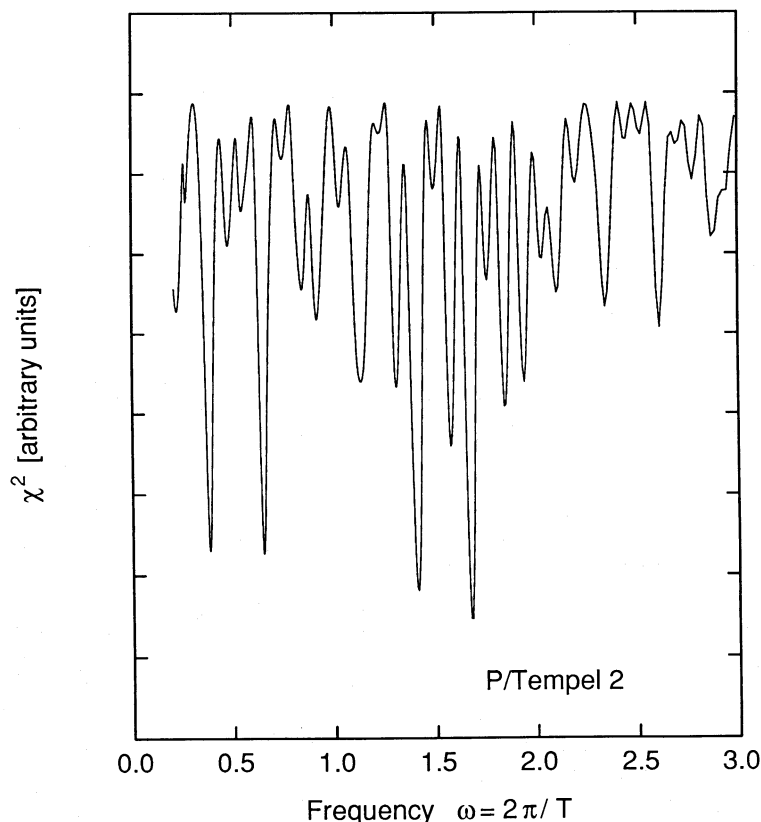


FIG. 5—Plot of χ^2 versus the angular frequency of the best-fitting two-peaked sinusoid, for comet P/Tempel 2 photometry

TABLE 7
SUMMARY OF PUBLISHED P/TEMPEL 2 PHOTOMETRY

Date	R (AU)	Δ (AU)	α	m_V	$m_R(1, 1, 0)^a$	Reference
1978 Oct 28	2.66	1.88	15°9	19.02 ± 0.1	14.39 ± 0.4	1 ^b
1978 Dec 22	2.97	2.10	8.6	18.5 ± 0.2	13.68 ± 0.2	2
1978 Dec 29	3.02	2.16	11.6	19.44 ± 0.2	14.41 ± 0.5	1 ^b
1979 Jan 28	3.19	2.68	16.6	18.40 ± 0.13	12.58 ± 0.1	3
1979 Jan 29	3.19	2.70	16.7	18.5 ± 0.3	12.66 ± 0.3	4
1979 Jan 31	3.20	2.74	16.9	18.65 ± 0.24	12.76 ± 0.3	3
1979 Feb 24	3.32	3.20	17.3	19.9 ± 0.2?	13.58 ± 0.2	4
1987 Mar 31—						
1987 Apr 03	3.99	3.17	9.3	19.5–19.8 ^c	13.6–13.9	5
1987 Mar 27	4.01	3.14	8.0	19.8	14.0	6
1987 Jan 25	4.19	3.40	8.9	20.0	13.9	7
1986 Dec 29	4.26	3.82	12.5	20.4	13.8	7

^a Absolute magnitude computed using $m_V - m_R = 0.5$ and $\beta = 0.04 \text{ mag deg}^{-1}$.

^b The listed error is the linear sum of the formal statistical error and a possible 0.3 mag systematic error in the photometry quoted by the authors.

^c Value of m_R is listed.

REFERENCES.—(1) Spinrad, Stauffer, and Newburn 1979; (2) Johnson, Smith, and Shorthill 1981; (3) Zellner, Tedesco, and Degewij 1979; (4) Barker, Cochran, and Rybski 1981; (5) This work; (6) Gehrels and Scotti 1987b; (7) Gehrels and Scotti 1987a.

phase coefficient, β (mag deg^{-1}), and the geometric albedo, p_R , determined in the cases of P/Arend-Rigaux and P/Neujmin 1 from combined optical/IR photometry (Campins, A'Hearn, and McFadden 1987; Millis, A'Hearn, and Campins 1987) and in the case of P/Halley from direct measurements of the size of the nucleus (Sagdeev *et al.* 1986) combined with optical photometry. The geometric albedos of P/Encke and P/Tempel 2 have been arbitrarily set to $p_R = 0.04$. A comparably low albedo for P/Encke is compatible with its large phase coefficient (Jewitt and Meech 1987). The last two columns of Table 8 list r (km) [the radius of a circle having an area equal to the rotationally averaged cross section as calculated from $m_R(1, 1, 0)$ and p_R] together with a/b (the projected nucleus axis ratio estimated from Δm).

The four CCD-observed nuclei exhibit large photometric ranges, indicative of their grossly aspherical shapes. The nuclei are shown in Figure 6, where the absolute magnitude, $m_R(1, 1, 0)$, is plotted versus the photometric range, Δm . Also plotted in Figure 6 are 18 small main-belt asteroids (diameters $D \leq 30$ km) from Binzel and Mulholland (1983). The Binzel and Mulholland (1983) compilation is particularly useful for our purposes since it is apparently free from the sensitivity selection effects which afflict many previous light curve studies. The use of data pertaining to asteroids comparable in size to the comet nuclei, avoids confusion with size-correlated shape effects. Some of the plotted asteroids are slightly larger than the nuclei; however, there is no formally significant diameter-photometric range correlation for $D \leq 30$ km (Binzel 1984) so that no bias should be introduced. Figure 6 shows that the nucleus ranges are large compared to the ranges of main-belt asteroids of similar size.

Only two out of the 18 well-observed small asteroids have photometric ranges $\Delta m \geq 0.5$ mag whereas all four CCD nuclei have $\Delta m \geq 0.5$. The mean photometric range of the small asteroids is $\Delta m = 0.2 \pm 0.2$ mag, while that of the comets is $\Delta m = 0.8 \pm 0.2$ mag. According to Student's "*t*-test," the difference between the means is significant at the 1% level (i.e., probably significant). Strictly, the *t*-test provides an upper limit to the significance of the difference, since we do not know if the

asteroid and comet distributions are normal, as demanded by the *t*-test. However, according to the nonparametric Mann-Whitney "*U*-test," the comet and small main-belt asteroid samples are different at the 2.5% level. We conclude that there is evidence for a real difference between the mean photometric ranges of the observed comet nuclei and main-belt asteroids of similar size, implying that the nuclei are much less spherical than the asteroids. In support of this conclusion, we note that radar observations of comet IRAS-Araki-Alcock (IAA) (Goldstein, Jurgens, and Sekanina 1984) reveal an aspherical nucleus of average radius ~ 4 km and with an axis ratio near 2:1. The nucleus of comet IAA is plotted in Figure 6; the absolute magnitude was estimated from the quoted radius and an assumed geometric albedo $p = 0.04$ (see Table 8).

Limited evidence suggests that the planet-crossing (i.e., dynamically short-lived) asteroids are less spherical than the main-belt asteroids. Specifically, the mean photometric range of 20 Earth and Mars crossers is $\Delta m = 0.58 \pm 0.11$ mag (Binzel 1984), 2–3 times larger than the mean range of main-belt asteroids and comparable to the 0.8 ± 0.2 mag mean range of the cometary nuclei (see Fig. 6). The latter similarity is consistent with, but does not prove, a genetic relationship between the comets and some of the planet crossers. Orbital similarities among comets and planet-crossing asteroids independently suggest a common origin. Clearly, more observational work is needed to test this tantalizing suggestion.

It must be emphasized that we are aware of no selection effect which would have biased our attention toward nuclei with large photometric ranges. Indeed, the particular comets in this study were selected on the basis of their favorable positions in the sky, on the basis of our ability to locate them at the telescope, and because their observational histories led us to believe that their coma production would be small at the time of observation. None of these selection criteria provide an obvious bias toward highly irregular nuclei (however, see § IVb).

The rotation periods of the comets in Table 8 are long compared to the mean rotation period of main-belt asteroids, $T \approx 9 \pm 1$ hr (Dermott, Harris, and Murray 1984), but they

TABLE 8
PROPERTIES OF COMET NUCLEI

Comet	$m_R(1, 1, 0)$	Δm	T (hr)	β (mag deg ⁻¹)	P_R	r (km)	a/b
P/Halley	13.3 ± 0.1^a	1.0 ± 0.1	≥ 18	0.04^b	0.04^c	5.7	2.5
P/Arend-Rigaux	13.9 ± 0.1^d	0.7 ± 0.1	13.56 ± 0.16	0.04^b	$0.03^{e,f}$	5.1	1.9
P/Neujmin 1	12.2 ± 0.2	0.5 ± 0.1	12.67 ± 0.05	0.034 ± 0.012	0.03 ± 0.01^g	10	1.6
P/Encke	14.3 ± 0.2^h	≥ 0.8	22.43 ± 0.08	0.04	0.04^b	3.7	≥ 2
P/Tempel 2	$\geq 13.6 \pm 0.1$	0.04	0.04^b	≤ 4.8	...
IAA	14.1	$0.7 \pm ?$	0.04^b	4^i	2^i

^a Meech, Jewitt, and Ricker 1986.

^b Assumed value.

^c Sagdeev *et al.* 1986.

^d Jewitt and Meech 1985.

^e Millis, A'Hearn, and Campins 1987.

^f Brooke and Knacke 1986.

^g Campins, A'Hearn, and Millis 1987.

^h Jewitt and Meech 1987.

ⁱ Goldstein, Jurgens and Sekanina 1984.

are *not* statistically different from the rotation periods of the small asteroids in the Binzel and Mullholland survey, basically because the asteroidal rotation period distribution is very broad. This is emphasized in Figure 7, where we have plotted the rotation period versus the equatorial axis ratio for small main-belt asteroids and for comet nuclei.

Figure 7 prompts the question "are the observed rotating, elongate nuclei stable against centripetal disruption?" For the sake of definiteness, we represent the nuclei by prolate spheroids in rotation about a minor axis; the nucleus of P/Halley is

approximately prolate spheroidal. Other choices of shape could be made but would be neither more nor less justified than the present one. The gravitational acceleration at the apex of a prolate spheroid is

$$g = -2\pi G\rho a \int_0^2 \left\{ \left[1 + f^2 \left(\frac{2}{s} - 1 \right) \right]^{-1/2} - 1 \right\} ds, \quad (7)$$

where $G = 6.67 \times 10^{-11}$ (N kg⁻² m²) is the gravitational constant, ρ (kg m⁻³) is the bulk density of the nucleus, a (m) is the

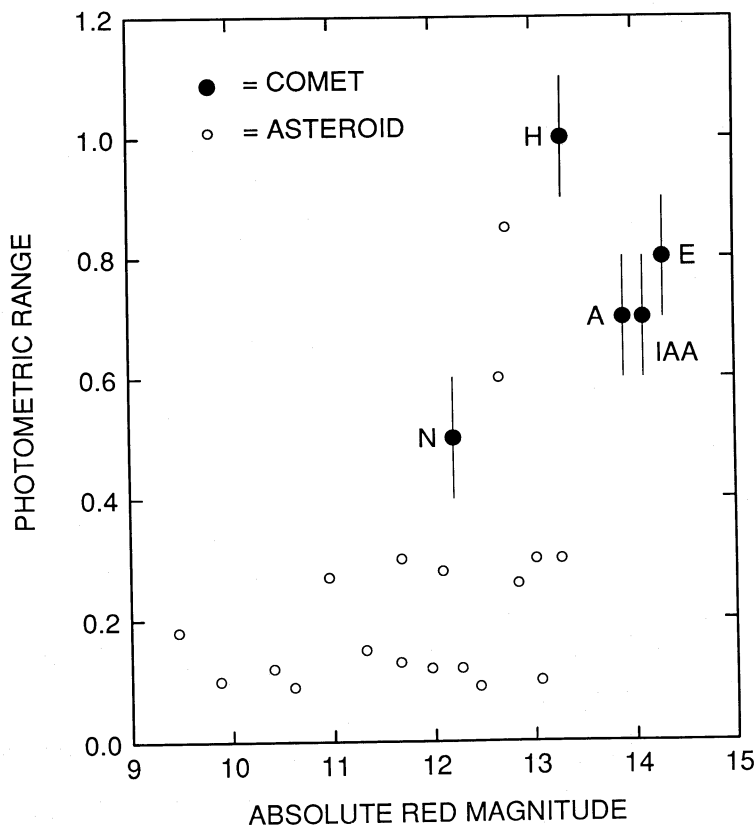


FIG. 6.—Plot of photometric range, Δm , versus absolute magnitude, $m_R(1, 1, 0)$, for small main-belt asteroids (empty circles) and comet nuclei (filled circles). The specific nuclei may be identified from the labels H = P/Halley, E = P/Encke, N = P/Neujmin 1, IAA = IRAS Aracki Alcock, and A = P/Arend-Rigaux. The figure shows that Δm for the nuclei is larger than Δm for typical small main-belt asteroids.

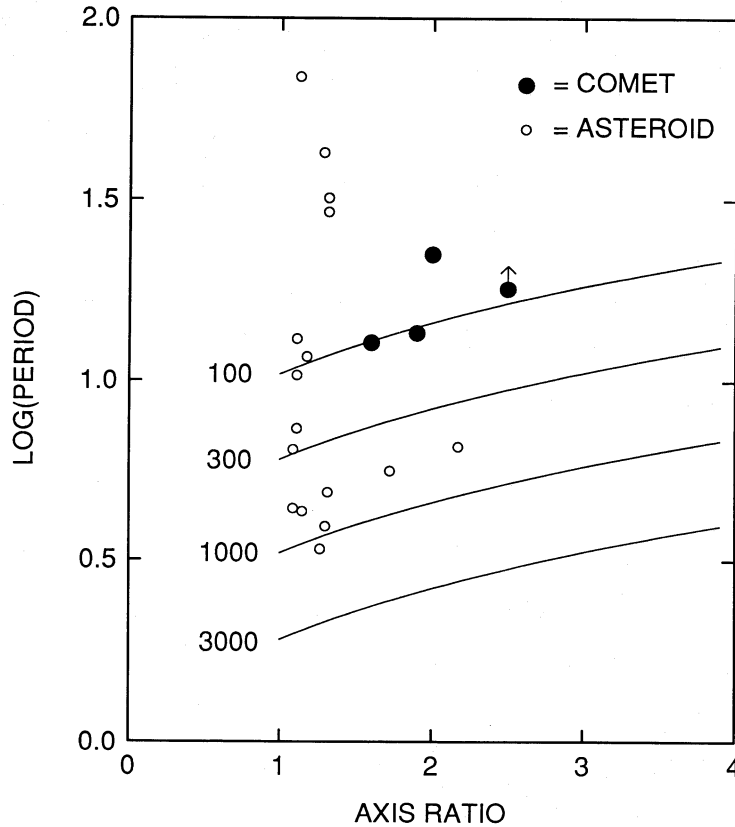


FIG. 7.—The logarithm of the rotation period in hours is plotted versus the axis ratio for small main-belt asteroids (*empty circles*) and comet nuclei (*filled circles*). The period of P/Halley is currently uncertain, with popular estimates being ~ 2 and ~ 7 days; we have plotted a reliable lower limit ($P \geq 18$ hr) from Meech, Jewitt, and Ricker 1986. Also plotted are model curves showing the critical period (eq. [7] and [8]) for prolate spheroidal nuclei with densities 100, 300, 1000, and 3000 kg m^{-3} .

semimajor axis, $f = b/a$ is the ratio of the semiminor to the semimajor axes, and s is fractional distance along the major axis in units of a . The critical rotation period at which the centripetal acceleration is equal to the gravitational acceleration, g (m s^{-2}), is

$$T_c = 2\pi \left(\frac{a}{g} \right)^{1/2}. \quad (8)$$

For example, a spherical body ($f = 1$) with $\rho = 1000 \text{ kg m}^{-3}$ has $T_c = 3.3$ hr; the regolith on such a body would be gravitationally unbound if the rotation period were less than 3.3 hr. For smaller densities, ρ , and aspherical nuclei, $f < 1$, the critical period T_c will adopt larger values.

Equations (7) and (8) are used to plot $\log_{10}(T_c)$ versus $1/f$ in Figure 7, for bulk densities $\rho = 100, 300, 1000,$ and 3000 kg m^{-3} . Only the density of the nucleus of P/Halley is observationally constrained; its density is $\rho = 100\text{--}200 \text{ kg m}^{-3}$ (Whipple 1986), about the same as that of light terrestrial snow. It may be seen that the nuclei fall either close to or above the curve for $\rho = 100 \text{ kg m}^{-3}$, showing that the nuclei are gravitationally bound, even if their densities are as low as the density of the nucleus of P/Halley. However, two nuclei (P/Arend-Rigaux and P/Neujmin 1) fall practically on the curve for $\rho = 100 \text{ kg m}^{-3}$, suggesting that centripetal effects may be important. Specifically, if these nuclei had rotation periods half their present values they would exist in a state of internal tensile stress, and might, depending on their tensile strength, break up. Spontaneous rupture of cometary nuclei is appar-

ently common: over 20 “split comets” have been recorded to date (Sekanina 1982). Centripetal break up, perhaps driven by torques from the mass loss, constitutes a simple and natural mechanism of nucleus splitting, in view of the low densities, elongate shapes, and probable aggregate structures of the nuclei.

IV. SHAPES

Why do the cometary nuclei appear more elongated than main-belt asteroids of similar size? Three possible explanations, discussed in following sections, come to mind: (1) the shape difference may be a projection effect due to a misalignment between the cometary rotation axis and the axis of maximum moment of inertia, (2) the shapes of the nuclei may have been altered by anisotropic mass loss, and (3) the shapes may reflect the different collisional histories of the comets and the asteroids. Naturally, the three possibilities may occur singly or in combination.

a) Projection Effect

A systematic difference may exist between the states of rotation of asteroids and those of cometary nuclei. In asteroids, the rotation vector is generally coincident with the axis of maximum moment of inertia, since this represents a minimum-energy rotation state. This state is probable because the time scale for collisions among asteroids (which tend to misalign the rotation and the axis of maximum moment of inertia) is greater than the time scale for damping due to internal dissipation

(Burns and Safronov 1973). In comets, however, the rotation vector may be misaligned from the axis of maximum moment of inertia by torques induced by noncentral mass loss in previous orbits. We estimate that the appropriate damping time for cometary nuclei is of order 10^6 yr, considerably greater than the time scale for the action of the sublimation torques (few 100 or few 1000 yr, depending on the orbit and lifetime of the comet when in the inner solar system). Thus, a triaxial comet nucleus (axes $a > b > c$) would give a systematically larger light curve range than would an asteroid of identical shape, due to the different rotation state (in a prolate nucleus, like P/Halley, the effect would be much smaller). The hypothesis, while plausible, can only be tested using future determinations of the shapes and rotation states of nuclei. This is the most mundane explanation of Figure 6.

b) Anisotropic Mass Loss

The shapes of the nuclei may have been changed in the recent past by anisotropic mass loss due to sublimation or to nucleus splitting. The effect is reminiscent of the change one induces in the shape of a spherical apple by eating down to the core. Anisotropic sublimation is *expected* even on an initially uniform, spherical nucleus, due to seasonal effects. Anisotropy of the mass loss is observationally suggested in many comets (including Halley's see Sagdeev *et al.* 1986; Keller *et al.* 1986) by the presence of asymmetrical fan and jet structures in the inner coma.

This explanation is attractive, not least because the comets of the present study are dynamically old, trapped in the inner solar system, and subjected to high insolation for many tens or hundreds of orbits (e.g., see Carusi *et al.* 1985). However, in order for this explanation to be viable, the comets must satisfy $t_s \leq t_d$, where t_s is the nucleus sublimation lifetime and t_d is the dynamical lifetime of the comet in the inner solar system. It is by no means clear that this condition is satisfied by the present comets, since both t_s and t_d are difficult to estimate even to the order of magnitude. For instance, calculation of t_s is difficult due to the growth and sporadic local disruption of a surface crust composed of refractory debris; the crust reduces the mass-loss rate far below the level expected from equilibrium sublimation of an exposed dirty ice surface. The dynamical time t_d is determined by the particular cometary orbit and by the interactions of each nucleus with the inner planets. The obvious test of the importance of anisotropic mass loss would be to ascertain whether the nuclei of dynamically new comets show systematically smaller a/b than do the nuclei of old comets.

c) Collisional Histories

Whereas the primordial physical properties of asteroids (e.g., shape, rotation period, rotation pole) are likely to have been modified by recent collisions, the corresponding properties of comet nuclei are unlikely to have been so changed. This is because the comets reside in the distended Oort Cloud, with a collision time much in excess of the age of the universe. The smaller asteroids, on the other hand, have collision times less than the age of the solar system. Moreover, the velocity dispersion among the asteroids is $\Delta v \approx 5 \text{ km s}^{-1}$, so that collisions between small asteroids tend to be erosive, in contrast to the gentle collisions which presumably led to the accretion of comets from cometesimals. In fact, many of the asteroids in the Binzel and Mulholland (1983) survey may be collision fragments of larger bodies. Simply on the basis of the relative

collision times, it seems reasonable to conjecture that the shapes of the nuclei might be close to the shapes they acquired at the time of their formation, while the shapes of the asteroids reflect recent collisional modification. We find this to be the most intriguing of the possible explanations of Figure 6, and so we explore it in more detail.

Can the large axis ratios inferred in the comets of the present study be produced by random agglomeration of icy planetesimals in the early solar system? Clearly, an exact answer cannot be given, but the simple calculation described below suggests that agglomerated nuclei should *routinely* possess axis ratios as large as the ones observed.

We have made a simple numerical model in order to investigate the distribution of body shapes among three-dimensional agglomerated particles. The model assumes perfect sticking of a set of equidimensional particles ("cometesimals") incident from random directions on an initial seed particle. The calculation starts with the seed particle at the center of a three-dimensional array. The agglomerate is grown by using a random number generator to select one of the available empty sites adjacent to the seed. A new particle is added to the randomly selected site. The program then identifies all the empty sites adjacent to the new agglomerate and the random number generator is used to select one of the sites for the addition of a new particle. This process is repeated until a preselected maximum number of particles has been reached by random accumulation. Typically, agglomerates of $N = 10^3$ particles were grown.

Many of the agglomerates grown in this way exhibit a crudely triaxial, or sometimes pancake-like body shape, as may be seen from Figure 8, (Plates 16–18). The Figure shows a single $N = 10^3$ agglomerate viewed along three mutually orthogonal axes (one of them being aligned with the major axis of the agglomerate). Delicate finger-like structures are apparent on the external surfaces of the agglomerates (reminding us of the fractal like way in which the agglomerates grow); apart from these structures, the agglomerates resemble the potato-shape of the nucleus of P/Halley. Thus, at least to zeroth order, it seems that the present shapes of the nuclei are compatible with the shapes which would be required at formation, if the nuclei are simple agglomerates of smaller cometesimals. By implication, the small main-belt asteroids may have been smoothed by the sandblasting effect of numerous, recent, high-velocity collisions. Like the nuclei, the Jovian Trojan asteroids exist in a region where sizable hypervelocity collisions are rare. The mean photometric range of the Trojans is $\Delta m \geq 0.4 \pm 0.2$ mag (Hartmann *et al.* 1988), larger than the range of the main-belt asteroids but similar to the mean range of the present cometary nuclei. This observation is consistent with the notion that the main-belt asteroids are collisionally smoothed.

Our preliminary conclusion may be modified by the inclusion of additional physical effects not considered here. More detailed calculations should modify the sticking law to allow incident particles to roll across the surface of the agglomerate into the nearest potential minimum and probably should include in the potential a centripetal term due to rotation of the agglomerate. Inclusion of a size distribution would change our result only if the smallest particles in the distribution contained most of the mass. Otherwise, the basic shape of the agglomerate would be determined by the geometry in which the largest cometesimals come to rest against each other. In an extreme case, the properties of the body are determined by the two-largest particles, as in the binary model of elongate aster-

oid Hector (Weidenschilling 1980). However, these additional calculations would take us beyond the scope of the present work and, in any case, are probably not justified by the small size of the comet nucleus sample.

In our estimation, the three possibilities described above provide roughly equally plausible explanations for the systematically larger rotational ranges of the cometary nuclei apparent in Figure 6. Presumably, sublimation torques and asymmetric mass loss will have had less effect on the dynamically new nuclei, leaving primordial effects as the major influence on these bodies. Measurements of the shapes of dynamically new cometary nuclei would help to separate the relative importance of the three effects. We are currently engaged in attempts to measure the properties of the nuclei of several dynamically new comets at large heliocentric distances ($R \geq 10$ AU). These observations are at the very edge of what is attainable using current technology.

V. CONCLUSIONS

The nuclei of certain comets can be studied from the ground using charge-coupled device (CCD) photometry. Whereas direct investigations using spacecraft are limited in number by the large costs and long planning times of spacecraft missions, CCD photometry can be applied to numerous nuclei in the near future at low cost. Specific conclusions of the present work are the following:

1. The nucleus of comet P/Neujmin 1 has been observed with a charge-coupled device at heliocentric distances $R = 3.88, 5.04,$ and 6.46 AU. The nucleus has absolute red ($\lambda \approx 0.65 \mu\text{m}$) magnitude $m_R(1, 1, 0) = 12.0 \pm 0.2$ at maximum light (0.2 – 0.3 mag fainter when rotationally averaged), phase coefficient $\beta = 0.034 \pm 0.012$ mag deg $^{-1}$ red geometric albedo $p_R = 0.03 \pm 0.01$, probable rotation period $T = 12.67 \pm 0.05$ hr, photometric range $\Delta m = 0.5 \pm 0.1$ mag, and equatorial axis ratio $a/b \geq 1.6$.

2. Comet P/Tempel 2 has been similarly observed at $R = 3.99$ AU, but its corresponding nucleus parameters are

less certain, since a coma may contaminate the P/Tempel 2 photometry. The limit to the absolute magnitude of the nucleus estimated from the present photometry is $m_R(1, 1, 0) \geq 13.6 \pm 0.1$. Nonrandom photometric variations of range $\Delta m \geq 0.3$ mag were observed.

3. The photometric ranges of the nuclei of comets P/Arend-Rigaux (0.7 mag), P/Neujmin 1 (0.5 mag), P/Halley (1.0 mag), and P/Encke (≥ 0.8 mag) are large compared to the typical ranges of main-belt asteroids of similar size (~ 0.2 mag). It is inferred that the nuclei are less spherical than main-belt asteroids of comparable size.

4. Three explanations of the aspherical nuclei seem about equally plausible. First, misalignment between the rotation vector and the axis of maximum moment of inertia induced by sublimation torques will cause triaxial comet nuclei to exhibit larger light curve ranges than do asteroids of identical shape. Misalignment could be caused by noncentral mass loss due to sublimation. Second, asphericity may be produced by anisotropic mass loss due to irregular sublimation or due to nucleus splitting. Third, the aspherical shapes of the nuclei may be primordial while the shapes of main-belt asteroids have presumably been modified (rounded) by numerous recent collisions. Future measurements will be needed to discriminate among these possibilities.

5. If the nuclei of all comets have densities as low as the density of the nucleus of P/Halley ($\rho \approx 100 \text{ kg m}^{-3}$), and if rotation is in the minimum energy state, then many nuclei must be rotating at or close to the centripetal limit.

We thank our telescope operators Dean Hudek, Dave Chamberlain, and Don Martin. Bill Schoenings' nightly attempts to relieve mechanical stress from the primary of the 2.1 m telescope are much appreciated. We thank Mike A'Hearn and Richard Binzel for thoughtful comments on this manuscript. This work was supported by a National Science Foundation grant to D. C. J. and by a NASA Graduate Researcher Award to K. J. M.

REFERENCES

- Barker, E. S., Cochran, A. L., and Rybski, P. M. 1981, in *Modern Observational Techniques for Comets*, ed. J. C. Brandt, B. Donn, J. M. Greenberg, and J. Rahe, (JPL Pub. 81-68).
- Binzel, R. P. 1984, *Icarus*, **57**, 294.
- Binzel, R. P., and Mulholland, J. D. 1983, *Icarus*, **56**, 519.
- Birkett, C. M., Green, S. F., Zarnecki, J. C., and Russell, K. S. 1987, *M.N.R.A.S.*, **225**, 285.
- Bowell, E., and Lumme, K. 1979, *Asteroids*, ed. T. Gehrels (Tucson: University of Arizona Press), p. 132.
- Brooke, T. Y., and Knacke, R. F. 1986, *Icarus*, **67**, 80.
- Burns, J. A., and Safronov, V. S. 1973, *M.N.R.A.S.*, **165**, 403.
- Campins, H., A'Hearn, M. F., and McFadden, L. 1987, *Ap. J.*, **316**, 847.
- Carusi, A., Kresak, L., Perozzi, E., and Valsecchi, G. B. 1985, *Long-term Evolution of Short Period Comets* (Bristol: Adam Hilger).
- Christian, C. A., Adams, M., Barnes, J. V., Butcher, H., Hayes, D. S., Mould, J. R., and Siegel, M. 1985 *Pub. A.S.P.*, **97**, 363.
- Dermott, S. F., Harris, A. W., and Murray, C. D. 1984, *Icarus*, **57**, 14.
- Dworetzky, M. M. 1983, *M.N.R.A.S.*, **203**, 917.
- Gehrels, T., and Scotti, J. 1987a, *IAU Circ. No.*, 4312.
- . 1987b, *Minor Planet Circ. No.* 11782.
- Goldstein, R. M., Jurgens, R. F., and Sekanina, Z. 1984, *A.J.*, **89**, 1745.
- Hartmann, W. K., Tholen, D. J., Goguen, J., Binzel, R. P., and Cruikshank, D. P. 1988, *Icarus*, in press.
- Jewitt, D. C., and Danielson, G. E. 1984, *Icarus*, **60**, 435.
- Jewitt, D. C., and Meech, K. J. 1985, *Icarus*, **64**, 329.
- . 1987, *A.J.*, **93**, 1542.
- Johnson, P. E., Smith, D. W., and Shorthill, R. W. 1981, *Nature*, **289**, 155.
- Keller, H. U., et al. 1986, In *Proc. of the 20th ESLAB Symposium on the Exploration of Halley's Comet*, Vol. 2, ed. B. Battrick, E. J. Rolfe, and R. Reinhard (Noordwijk: ESA), p. 359.
- Meech, K. J., Jewitt, D. C., and Ricker, G. R. 1986, *Icarus*, **66**, 561.
- Marsden, B. G. 1968, *A.J.*, **73**, 367.
- Millis, R., A'Hearn, M. F., and Campins, H. 1987, preprint.
- Sagdeev, R., et al. 1986, In *Proc. of the 20th ESLAB Symposium on the Exploration of Halley's Comet*, Vol. 2, ed. B. Battrick, E. J. Rolfe, and R. Reinhard (Noordwijk: ESA), p. 317.
- Sekanina, Z. 1976, in *The Study of Comets Part III, A Continuing Controversy: Has the Cometary Nucleus Been Resolved?* ed. B. Donn, M. Mumma, W. Jackson, M. A'Hearn, and R. Harrington, (NASA SP 393), p. 537.
- . 1982 in *Comets*, ed. L. L. Wilkening (Tucson: University of Arizona Press), p. 251.
- Spinrad, H., Stauffer, J., and Newburn, R. L. 1979, *Pub. A.S.P.*, **92**, 707.
- Tedesco, E. F., and Barker, E. S. 1981, in *IAU Colloquium 61, Comets: Gases, Ices, Grains, and Plasma* ed. L. Wilkening (Tucson: University of Arizona Press).
- Tokunaga, A. T., and Hanner, M. S. 1985, *Ap. J. (Letters)*, L13.
- Weidenschilling, S. J. 1980, *Icarus*, **44**, 807.
- Whipple, F. L. 1986, *Proc. of the 20th ESLAB Symposium on the Exploration of Halley's Comet*, Vol. 2, ed. B. Battrick, E. J. Rolfe, and R. Reinhard (Noordwijk: ESA), p. 281.
- Wisniewski, W. Z., Fay, T., and Gehrels, T. 1986, *Asteroids, Comets, Meteors II*, ed. C. Lagerkvist, B. Linblad, H. Lundstedt, and H. Rickman, (Uppsala: Uppsala University Press), p. 337.
- Yeomans, D. K. 1978, *Comet Tempel 2 Orbit Ephemerides, and Error Analysis* (JPL Pub. 78-85).
- Zellner, B., Tedesco, E., and Degewij, J. 1979, *IAU Circ. No.* 3326.

DAVID JEWITT: 54-418 MIT, Cambridge, MA 02139

KAREN MEECH: Institute for Astronomy, University of Hawaii, 2680 Woodlawn Drive, Honolulu, HI 96822

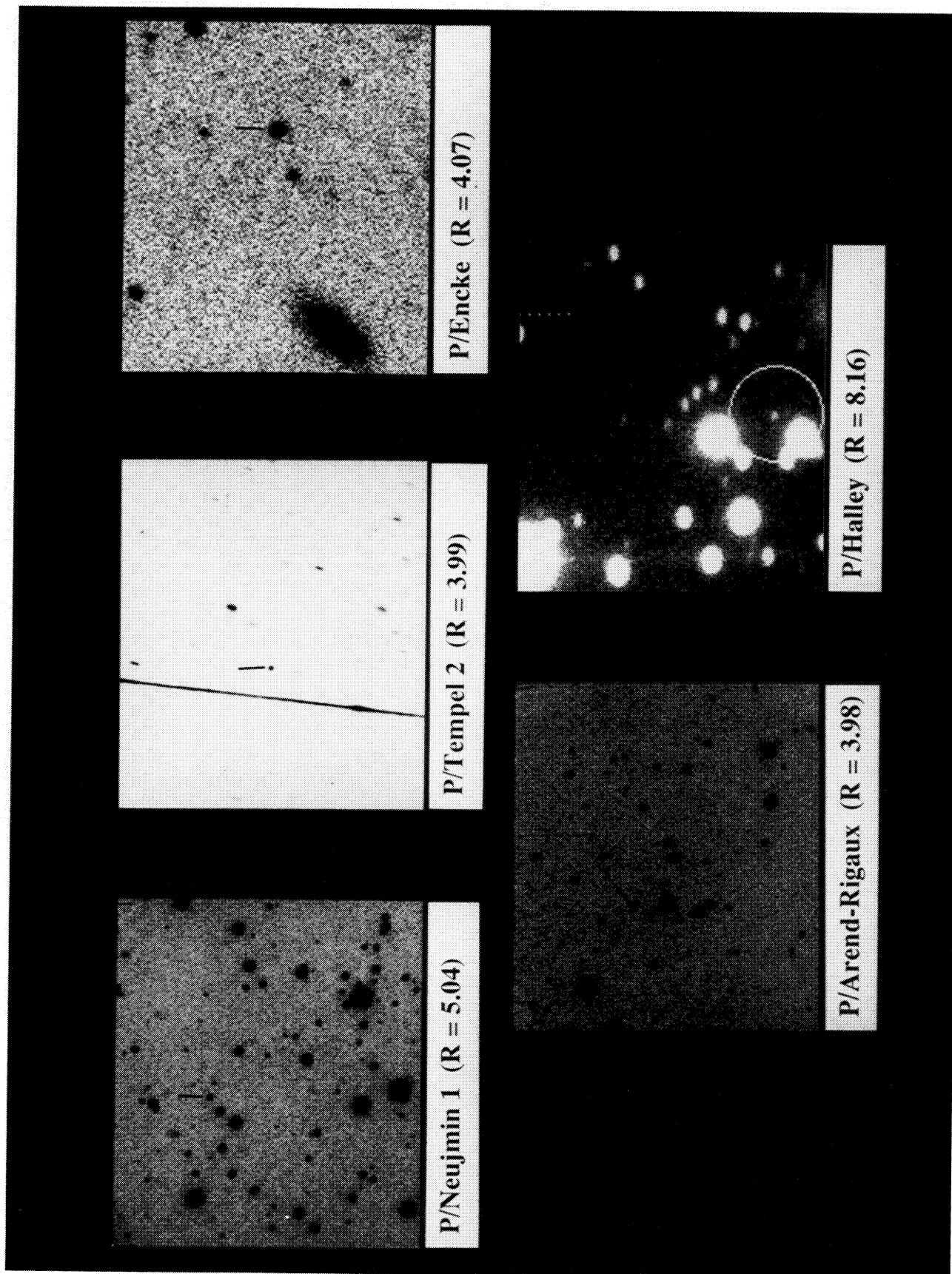


FIG. 1.—CCD images of the point source comets discussed in this work. The images are roughly $1'$ on a side and show (a) comet P/Neujmin 1, (b) comet P/Tempel 2, (c) comet P/Encke, (d) comet P/Arend-Rigaux, and (e) comet P/Halley. The heliocentric distances of the comets at the times of observation are indicated. The dark line near the image of Tempel 2 is a meteor trail.

JEWITT AND MEECH (see 328, 975)

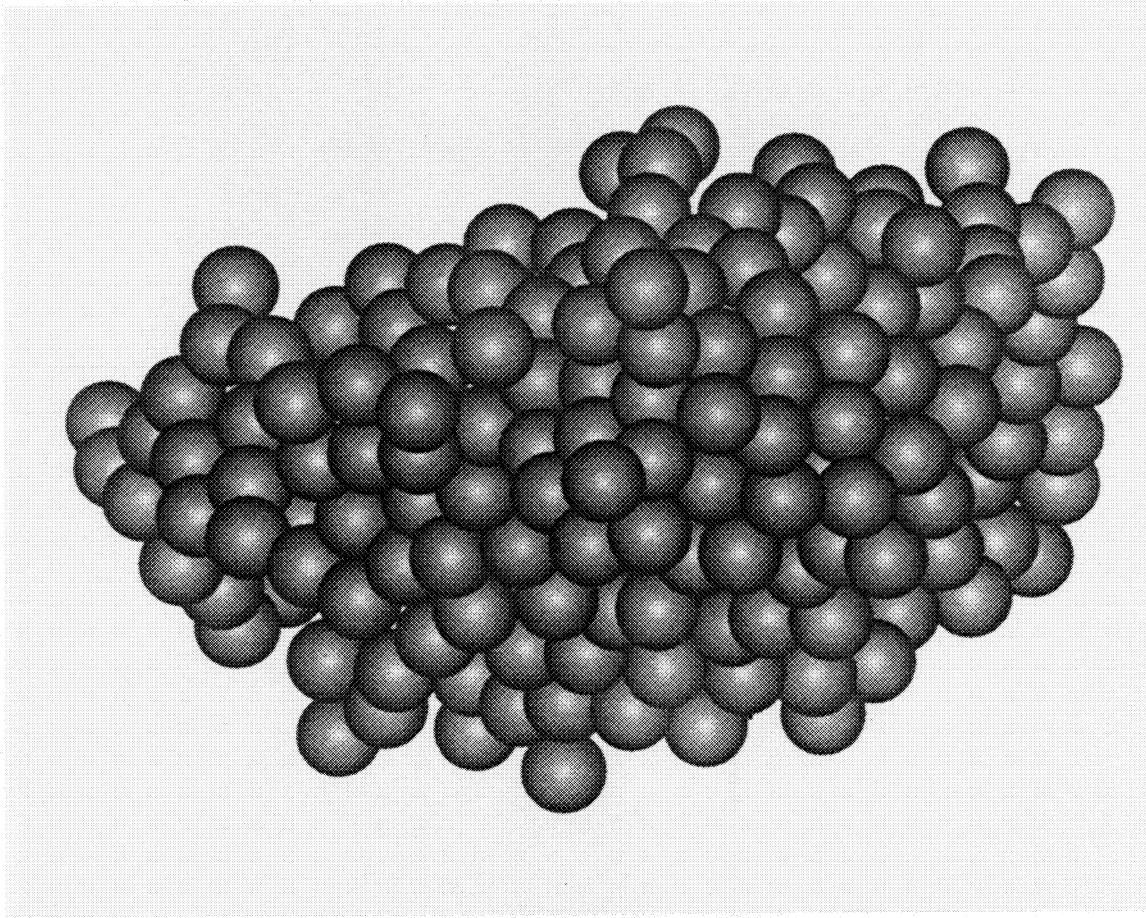


FIG. 8a

FIG. 8.—Three views of a typical random aggregate along mutually orthogonal directions are shown in (a), (b), and (c). The aggregate contains $N = 10^3$ particles and was grown according to the procedure described in § IVc. The aspherical shape of the aggregate is a result of chance and is comparable to the shapes of the cometary nuclei as inferred from the present CCD photometry.

JEWITT AND MEECH (see 328, 985)

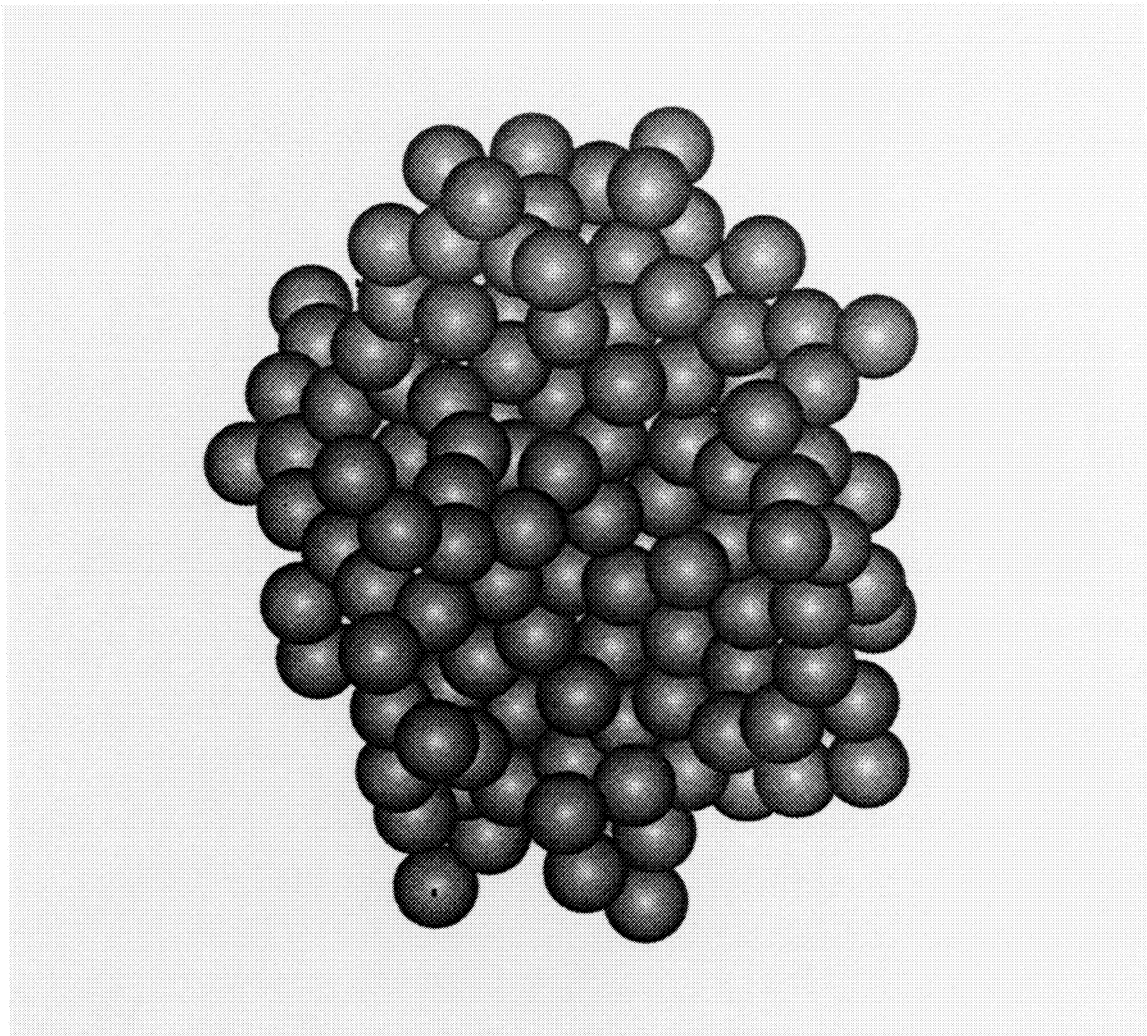


FIG. 8b

JEWITT AND MEECH (see 328, 985)

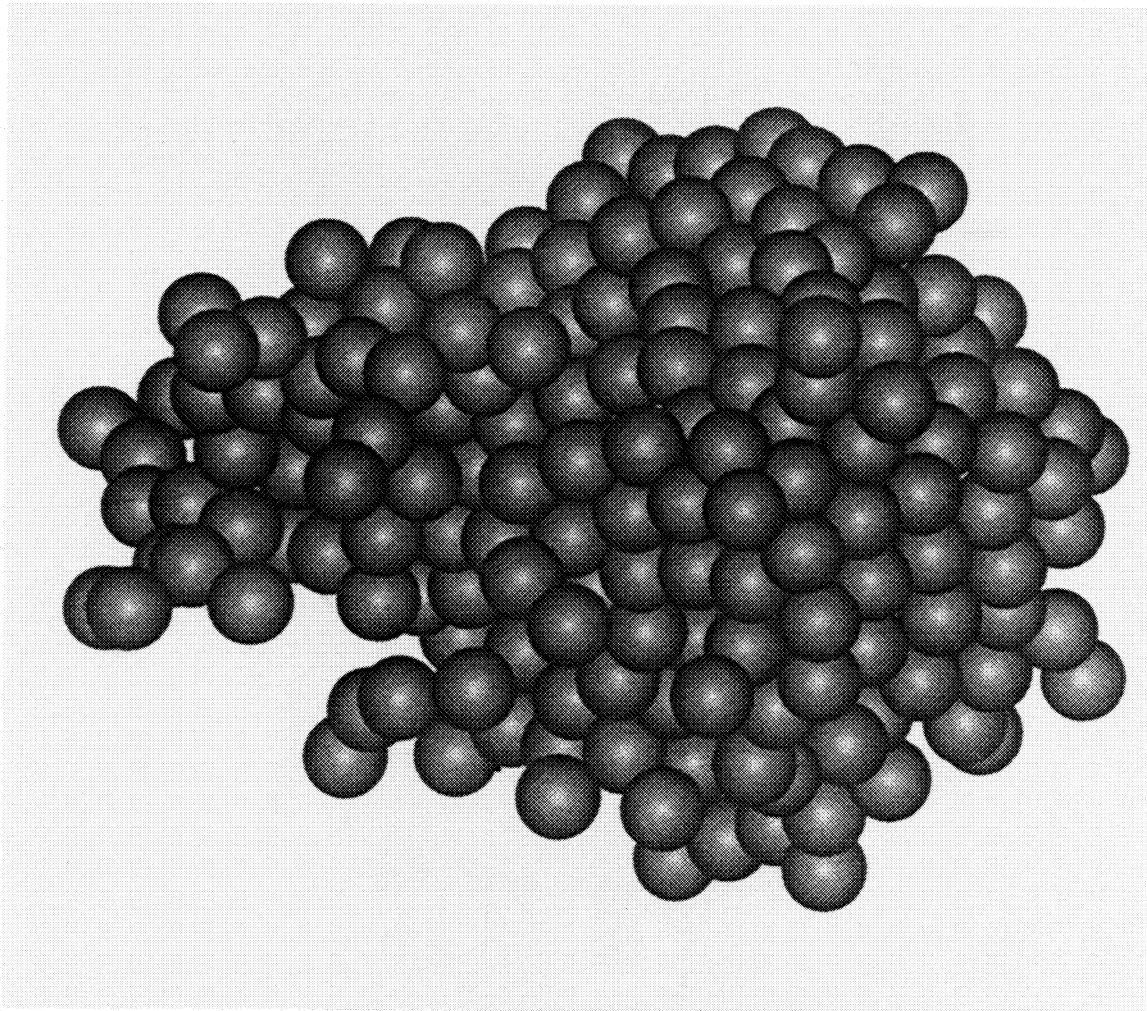


FIG. 8c

JEWITT AND MEECH (see 328, 985)